Inorganic Chemistry
Article

Inorg. Chem. **2010**, *49*, 8025–8033 **8025**
DOI: 10.1021/ic101054u

Mechanism of Nitric Oxide Reactivity and Fluorescence Enhancement of the NO-Specific Probe CuFL1

Lindsey E. McQuade, Michael D. Pluth, and Stephen J. Lippard*

Department of Chemistry, Massachusetts Institute of Technology, Cambridge, Massachusetts 02139

Received May 24, 2010

The mechanism of the reaction of CuFL1 (FL1 = 2-{2-chloro-6-hydroxy-5-[(2-methylquinolin-8-ylamino)methyl]-3-oxo-3*H*-xanthen-9-yl}benzoic acid) with nitric oxide (NO) to form the N-nitrosated product FL1-NO in buffered aqueous solutions was investigated. The reaction is first-order in [CuFL1], [NO], and [OH^-]. The observed rate saturation at high base concentrations is consistent with a mechanism in which the protonation state of the secondary amine of the ligand is important for reactivity. This information provides a rationale for designing faster-reacting probes by lowering the pK_a of the secondary amine. Activation parameters for the reaction of CuFL1 with NO indicate an associative mechanism ($\Delta S^{\ddagger} = -120 \pm 10$ J/mol·K) with a modest thermal barrier ($\Delta H^{\ddagger} = 41 \pm 2$ kJ/mol; $E_a = 43 \pm 2$ kJ/mol). Variable-pH electron paramagnetic resonance experiments reveal that, as the secondary amine of CuFL1 is deprotonated, electron density shifts to yield a new spin-active species having electron density localized on the deprotonated amine nitrogen atom. This result suggests that FL1-NO formation occurs when NO attacks the deprotonated secondary amine of the coordinated ligand, followed by inner-sphere electron transfer to Cu(II) to form Cu(I) and release of FL1-NO from the metal.

Introduction

Nitric oxide (NO), once thought to be an environmental pollutant, is now recognized as an important biological signaling molecule that is responsible for cardiac function,[1−5] neurotransmission,[6−8] and fighting invading pathogens during an immune response.[9,10] The lifetime of NO in solution varies depending on conditions,[11,12] and nitrosated species such as *S*-nitrosothiols and *N*-nitrosamines are proposed to act as vehicles for NO storage and transport in biology.[13,14] Transition metals are also major targets of NO attack, with the classic example being nitrosylation of the heme iron of soluble guanylyl cyclase to effect downstream vascular smooth muscle dilation.[15] NO can reductively nitrosylate metals, effecting one-electron reduction of the metal and nitros(yl)ation of a nucleophile by the resulting NO^+ to form an E−NO species, where E is O, N, or S.[16] This chemistry provides a mechanism by which metal complexes react with NO,[16−19] and it has also been employed as a strategy for NO sensing by transition-metal-based sensors.[20−30]

*To whom correspondence should be addressed. E-mail: lippard@mit.edu.

(1) Furchgott, R. F.; Vanhoutte, P. M. *FASEB J.* **1989**, *3*, 2007–2018.
(2) Ignarro, L. J.; Buga, G. M.; Wood, K. S.; Byrns, R. E.; Chaudhuri, G. *Proc. Natl. Acad. Sci. U.S.A.* **1987**, *84*, 9265–9269.
(3) Rapoport, R. M.; Draznin, M. B.; Murad, F. *Nature* **1983**, *306*, 174–176.
(4) Palmer, R. M. J.; Ferrige, A. G.; Moncada, S. *Nature* **1987**, *327*, 524–526.
(5) Bolotina, V. M.; Najibi, S.; Palacino, J. J.; Pagano, P. J.; Cohen, R. A. *Nature* **1994**, *368*, 850–853.
(6) Garthwaite, J. *Eur. J. Neurosci.* **2008**, *27*, 2783–2802.
(7) Bredt, D. S.; Hwang, P. M.; Snyder, S. H. *Nature* **1990**, *347*, 768–770.
(8) Shibuki, K.; Okada, D. *Nature* **1991**, *349*, 326–328.
(9) Bogdan, C. *Nat. Immunol.* **2001**, *2*, 907–916.
(10) Marletta, M. A.; Yoon, P. S.; Iyengar, R.; Leaf, C. D.; Wishnok, J. S. *Biochemistry* **1988**, *27*, 8706–8711.
(11) Liu, X.; Miller, M. J. S.; Joshi, M. S.; Thomas, D. D.; Lancaster, J. R., Jr. *Proc. Natl. Acad. Sci. U.S.A.* **1998**, *95*, 2175–2179.
(12) Thomas, D. D.; Liu, X.; Kantrow, S. P.; Lancaster, J. R., Jr. *Proc. Natl. Acad. Sci. U.S.A.* **2001**, *98*, 355–360.
(13) Gladwin, M. T.; Schechter, A. N. *Circ. Res.* **2004**, *94*, 851–855.
(14) Vanin, A. F. *Biochemistry* (*Moscow, Russ. Fed.*) **1998**, *63*, 782–793.
(15) Cary, S. P. L.; Winger, J. A.; Derbyshire, E. R.; Marletta, M. A. *Trends Biochem. Sci.* **2006**, *31*, 231–239.
(16) Ford, P. C.; Fernandez, B. O.; Lim, M. D. *Chem. Rev.* **2005**, *105*, 2439−2455 and references cited therein.
(17) Melzer, M. M.; Mossin, S.; Dai, X.; Bartell, A. M.; Kapoor, P.; Meyer, K.; Warren, T. H. *Angew. Chem., Int. Ed.* **2010**, *49*, 904–907.
(18) Sarma, M.; Singh, A.; Gupta, G. S.; Das, G.; Mondal, B. *Inorg. Chim. Acta* **2010**, *363*, 63–70.
(19) Tran, D.; Skelton, B. W.; White, A. H.; Laverman, L. E.; Ford, P. C. *Inorg. Chem.* **1998**, *37*, 2505–2511.
(20) Khin, C.; Lim, M. D.; Tsuge, K.; Iretskii, A.; Wu, G.; Ford, P. C. *Inorg. Chem.* **2007**, *46*, 9323–9331.
(21) Lim, M. H.; Lippard, S. J. *J. Am. Chem. Soc.* **2005**, *127*, 12170–12171.
(22) Lim, M. H.; Lippard, S. J. *Inorg. Chem.* **2006**, *45*, 8980–8989.
(23) Lim, M. H.; Lippard, S. J. *Acc. Chem. Res.* **2007**, *40*, 41–51.
(24) Lim, M. H.; Wong, B. A.; Pitcock, W. H., Jr.; Mokshagundam, D.; Baik, M.-H.; Lippard, S. J. *J. Am. Chem. Soc.* **2006**, *128*, 14364–14373.
(25) Lim, M. H.; Xu, D.; Lippard, S. J. *Nat. Chem. Biol.* **2006**, *2*, 375–380.
(26) Ouyang, J.; Hong, H.; Shen, C.; Zhao, Y.; Ouyang, C.; Dong, L.; Zhu, J.; Guo, Z.; Zeng, K.; Chen, J.; Zhang, C.; Zhang, J. *Free Radical Biol. Med.* **2008**, *45*, 1426–1436.
(27) Smith, R. C.; Tennyson, A. G.; Lim, M. H.; Lippard, S. J. *Org. Lett.* **2005**, *7*, 3573–3575.
(28) Smith, R. C.; Tennyson, A. G.; Won, A. C.; Lippard, S. J. *Inorg. Chem.* **2006**, *45*, 9367–9373.

Published on Web 08/12/2010

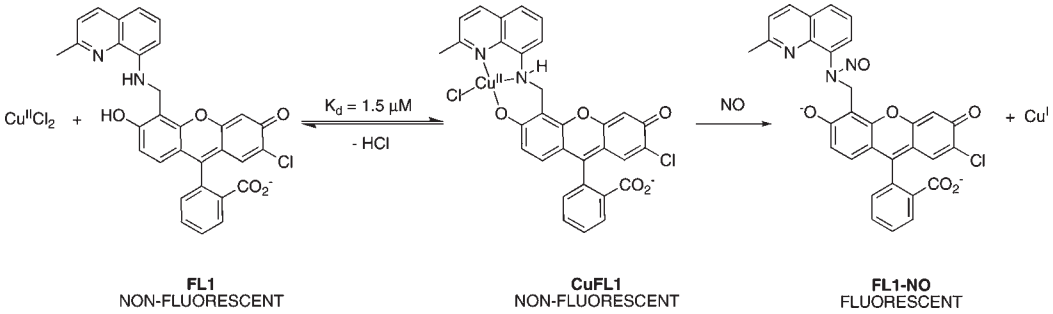

Figure 1. CuFL1 and its NO detection scheme.

Scheme 1. Proposed Mechanism 1 for the Reaction of CuFL1 with NO

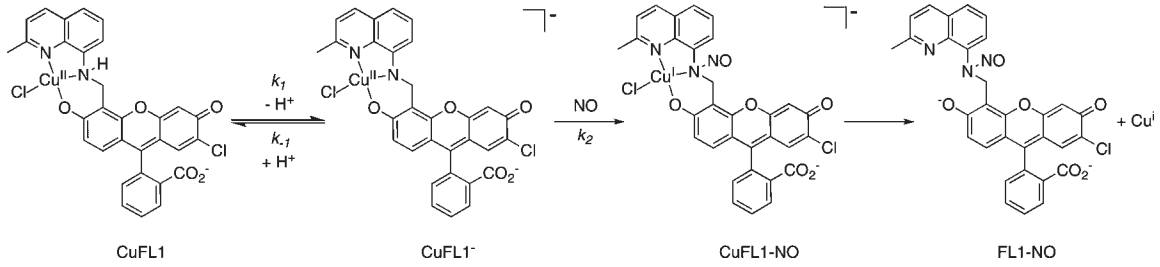

Recently, we reported one such NO-specific probe, CuFL1 (Figure 1).[24,25] The FL1 ligand is minimally fluorescent, and density functional theory (DFT) calculations revealed that quenching is due to photoinduced electron transfer from lone-pair electrons delocalized throughout the aminoquinaldine unit into the half-filled fluorescein molecular orbital in the excited state.[24] The fluorescence is further quenched by coordination to a paramagnetic Cu(II) ion. Treatment of a 1:1 mixture of FL1 and $CuCl_2$ in anaerobic buffered solutions with excess NO results in formation of a fluorescent species. Under similar anaerobic conditions, neither treatment of FL1 with NO nor addition of Cu(I) results in fluorescence enhancement. Upon exposure of CuFL1 to NO, Cu(II) is reduced to Cu(I), as evidenced by optical, electron paramagnetic resonance (EPR), and UV−vis spectroscopy, electrospray ionization mass spectrometry studies, and the independent synthesis of FL1-NO.[24,25] FL1-NO is highly emissive with a quantum yield of 0.58 ± 0.02, compared to those of FL1 ($\phi = 0.077 \pm 0.002$) and CuFL1 ($\phi = 0.063 \pm 0.002$). Formation of FL1-NO with concomitant reduction of Cu(II) to Cu(I) is therefore responsible for the fluorescence enhancement observed when minimally emissive CuFL1 reacts with NO (Figure 1). Such an emission enhancement mechanism is consistent with prior work[29] with a copper(II) dianthracenylcyclam complex, $[Cu(DAC)]^{2+}$. A more detailed mechanistic examination of $[Cu(DAC)]^{2+}$ suggested that NO reacts at a deprotonated secondary amine of the ligand with concomitant inner-sphere electron transfer to Cu(II) to produce Cu(I) and the nitrosated DAC-NO ligand as products.[20]

The reaction of CuFL1 with NO most likely proceeds through one of two possible mechanisms. The first, mechanism 1, is analogous to that proposed for $[Cu(DAC)]^{2+}$ and involves initial deprotonation of the secondary amine of the complexed ligand, followed by direct attack of NO at that site to form FL1-NO (Scheme 1), which would result in reduction of Cu(II) to Cu(I). The final step is release of the metal from FL1-NO, a poor ligand for the soft Cu(I) center because of its hard oxygen and nitrogen donor atoms, inability to conform to tetrahedral geometry, and lowered electron density on the nitrosamine. The second, mechanism 2, invokes the initial formation of a Cu(I)-NO complex (Scheme 2). Deprotonation of the secondary amine ligated to Cu(I)-NO would facilitate NO transfer from the metal to the ligand, again followed by the release of Cu(I) from FL1-NO.

In the present article, we present a kinetic and mechanistic investigation of the nitrosation of CuFL1 under varying conditions, including pH-dependent studies and an Eyring analysis, together with a spectroscopic evalution of the electronic structure of CuFL1. These mechanistic tools suggest a preferred reaction pathway for the chemistry that underlies the turn-on fluorescence of the sensor.

Experimental Section

Materials. 2-{2-Chloro-6-hydroxy-5-[(2-methylquinolin-8-ylamino)methyl]-3-oxo-3*H*-xanthen-9-yl}benzoic acid (FL1) was prepared by a previously reported procedure.[25] All other chemicals were used as received. Piperazine-*N*,*N*′-bis(2-ethanesulfonic acid) (PIPES) was purchased from Calbiochem, and potassium chloride (99.999%) was purchased from Aldrich. Buffer solutions (50 mM PIPES and 100 mM KCl, at pH 6.0, 6.5, 7.0, 7.5, 8.0, and 8.7) were prepared in Millipore water and used for all spectroscopic studies except for pK_a titrations and solvent isotope effect determinations. pK_a titrations were performed in a solution of 20 mM KOH and 100 mM KCl, at pH 12, in Millipore water. The pH of the solutions was adjusted using 6, 1, or 0.1 N HCl and 0.1 N KOH. Potassium carbonate (Mallinckrodt) was used as a buffer for solvent isotope effect determinations. Buffer solutions (20 mM K_2CO_3 and 100 mM KCl) were prepared at pH/D 7.0 in Millipore water or D_2O (Cambridge Isotope Laboratories), using a correction of 0.4 pH

(29) Tsuge, K.; DeRosa, F.; Lim, M. D.; Ford, P. C. *J. Am. Chem. Soc.* **2004**, *126*, 6564–6565.
(30) Xing, C.; Yu, M.; Wang, S.; Shi, Z.; Li, Y.; Zhu, D. *Macromol. Rapid Commun.* **2007**, *28*, 241–245.

Scheme 2. Proposed Mechanism 2 for the Reaction of CuFL1 with NO

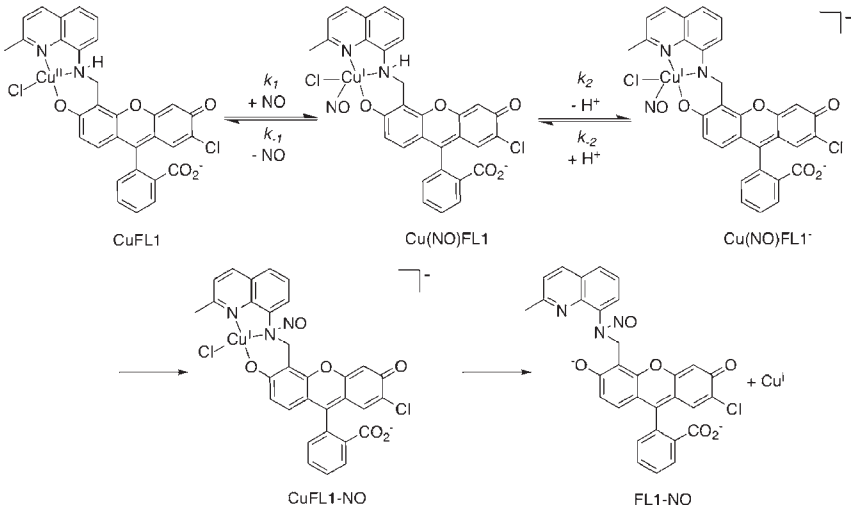

meter units to account for the differential readings of glass electrodes in D_2O.[31] For EPR experiments, solutions at pH 12.7 (50 mM KOH and 100 mM KCl), pH 10.1 (20 mM K_2CO_3 and 100 mM KCl), pH 7.0 (50 mM PIPES and 100 mM KCl), and pH 4.0 (20 mM NaOAc and 100 mM KCl; sodium acetate purchased from Aldrich) were prepared in Millipore water. Copper chloride dihydrate (99+%) was purchased from Alfa Aesar, and stock solutions of 10 and 1 mM were prepared in Millipore water. Stock solutions of 1 mM FL1 were prepared in dimethyl sulfoxide (DMSO) and stored in aliquots at −80 °C.

Kinetic Studies of the Reaction of CuFL1 with NO. Absorbance measurements were made under anaerobic conditions, with cuvette solutions prepared in an inert-atmosphere glovebox. Buffer and $CuCl_2$ solutions were sparged with dinitrogen with vigorous stirring overnight to remove dissolved oxygen prior to use and stored under an inert atmosphere. Aliquots of FL1 were thawed immediately prior to use, deoxygenated by applying 10 cycles of evacuation and backfill with dinitrogen to provide an inert atmosphere for sample preparation. Cuvette solutions were prepared by combining $CuCl_2 \cdot 2H_2O$ and FL1 in a 1:1 ratio in buffer and sealing the cuvette with a septum-equipped, gastight cap. NO was purchased from Airgas and purified as previously described to minimize contamination by higher nitrogen oxides.[32] NO gas was introduced into buffered solutions via gastight syringes. Samples were stirred throughout acquisitions to ensure equal distribution of NO throughout the sample solution. Acquisitions were made at 25.00 ± 0.05 °C unless otherwise noted. UV−vis spectra were acquired on a Cary 50-Bio spectrometer using spectrosil quartz cuvettes with gastight septa caps from Starna Cells Inc. (3.5 mL volume and 1 cm path length). Measurements were recorded over 45 min using the scanning kinetics program in *Cary WinUV* version 3.00, and changes in the intensity of the $\pi \rightarrow \pi^*$ transition of fluorescein at either 498 nm (decrease of CuFL1) or 504 nm (increase of FL1-NO) were monitored. The data were fit using *OriginPro 8* software, and a regression analysis was performed using *Microsoft Excel 2004*, version 11.5.6. All absorbance experiments were performed in triplicate. Fluorescence spectra for pK_a titrations were obtained on a Quanta Master 4 L-format scanning spectrofluorimeter (Photon Technology International) at 25.0 ± 0.1 °C.

EPR Measurements. EPR measurements were performed on a Bruker EMX EPR instrument at 9.33 GHz (X-band). EPR samples were prepared under anaerobic conditions in an inert-atmosphere glovebox. Stock solutions of 10 mM $CuCl_2$ and solutions of pH 12.7, 10.1, 7.0, and 4.0 were deoxygenated following standard procedures prior to use and stored under an inert atmosphere. Stock solutions of 5 mM FL1 were prepared in DMSO and stored in aliquots at −80 °C. Aliquots were thawed immediately prior to use, deoxygenated using standard procedures, and brought under an inert atmosphere for sample preparation. Samples were prepared by combining $CuCl_2$ and FL1 to final concentrations of 400 and 500 μM, respectively, such that 98.6% of Cu(II) was bound (determined from K_d(CuFL1) = 1.5 μM).[24,25] Spectra were recorded as a frozen glass (8−10% DMSO in water). Spectra were reported from four scans with a time constant of 2.56 ms, a modulation amplitude of 10 G, and a microwave power of 2.01 mW. Samples were thawed and brought back under an inert atmosphere, and 500 μL of NO was introduced to the samples via a gastight syringe. The samples were shaken to distribute NO throughout the solutions and then allowed to react at room temperature overnight (~13 h) in the dark. Samples were refrozen into a glass prior to recording their post-NO-treatment EPR spectra. Spectra were analyzed using the WINEPR System 2.11b.

Results and Discussion

Kinetic Studies of the Reaction of CuFL1 with NO. When anaerobic buffered solutions of CuFL1 were exposed to excess NO under pseudo-first-order conditions, the electronic spectra changed temporally as expected from previous work.[25] The CuFL1 band at 498 nm ($\pi \rightarrow \pi^*$ fluorescein transition) decreased slowly with concomitant growth of a new band at 504 nm corresponding to FL1-NO (Figure S1 in the Supporting Information, SI). Well-anchored isosbestic points at 500 and 524 nm were observed, suggesting the formation of one spectroscopically observable product. A plot of the absorbance at 504 nm versus time revealed a rise in product formation (Figure S1, inset, in the SI), which fit well to a first-order exponential equation (Figure S1, inset, in the SI), and such fittings were used to determine the observed rate constants (k_{obs}) for the reactions.

Determining the Rate Equation for the Reaction of CuFL1 with NO. Increases in [CuFL1],[33] [NO], and pH all accelerated the rate of FL1-NO formation. To determine the reaction order in [CuFL1], kinetic data were

(31) Glasoe, P. K.; Long, F. A. *J. Phys. Chem.* **1960**, *64*, 188–190.
(32) Lim, M. D.; Lorkovic, I. M.; Ford, P. C. *Methods Enzymol.* **2005**, *396*, 3–17.

(33) [CuFL1] = [Cu(II)] = [FL1] and assumes no dissociation of Cu(II) from the complex.

Table 1. Kinetic Parameters for the Reaction of CuFL1 with NO[a]

[CuFL1] (μM)[b]	k_{obs} (s^{-1})[c]	[NO] (μM)[d]	k_{obs} (s^{-1})	pH[e]	k_{obs} (s^{-1})[f]
2	0.0022(5)	650	0.0040(3)	6.0	0.00068(6)
3	0.00324(9)	975	0.0046(6)	6.5	0.0017(2)
4	0.0040(3)	1300	0.008(2)	7.0	0.0039(3)
5	0.006(1)	1950	0.012(3)	7.5	0.008(2)
6	0.0072(9)	2600	0.014(4)	8.0	0.011(4)
				8.7	0.014(6)

[a] Measurements were performed in 50 mM PIPES, 100 mM KCl, T = 25 °C. [b] [NO] = 650 μM. [c] k_{obs} values were determined by fitting the absorbance at 504 nm versus time to a single-exponential equation, $y = Ae^{-x/t} + y_0$. [d] [CuFL1] = 4 μM. [e] [CuFL1] = 4 μM; [NO] = 650 μM. [f] k_{obs} values were determined by fitting the absorbance at 498 nm for pH 6.0 and 6.5.

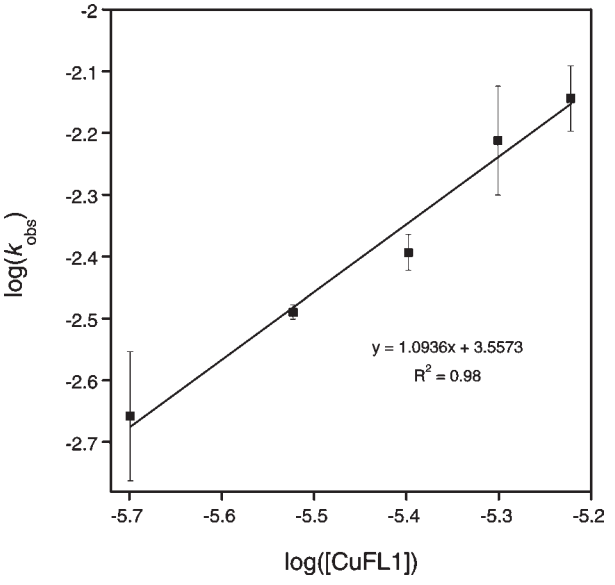

Figure 2. Plot of $\log(k_{obs})$ vs log([CuFL1]) for the reactions of 2−6 μM CuFL1 with 650 μM NO in 50 mM PIPES and 100 mM KCl at pH 7.0. T = 25 °C.

collected at constant pH, NO concentration, and temperature. A greater than 100-fold excess of NO (650 μM) was used to maintain pseudo-first-order conditions. The observed pseudo-first-order rate constants are summarized in Table 1, left-hand columns. A plot of the k_{obs} values versus the concentration of CuFL1 revealed a linear relationship, and the corresponding log/log plot of k_{obs} versus [CuFL1] revealed a CuFL1 reaction order of unity (1.09 ± 0.09 after linear regression; Figure 2). Although every effort was made to exclude dioxygen from the reaction, there is possible dioxygen leakage into the cuvettes over time, which differentially affects the reactions based on their rate. Therefore, the most likely source of error in the measurements is the NO concentration, which varies if dioxygen is present because of the formation of higher nitrogen oxides. Despite this systematic error, the slope of the log/log plot clearly indicates a first-order dependence on the concentration of CuFL1.

To determine the reaction order in NO concentration, kinetic data were collected at constant pH, CuFL1 concentration, and temperature (Table 1, middle columns). Again, a greater than 100-fold excess of NO was used

(34) Shaw, A. W.; Vosper, A. J. *J. Chem. Soc., Faraday Trans.* **1977**, *73*, 1239–1244.

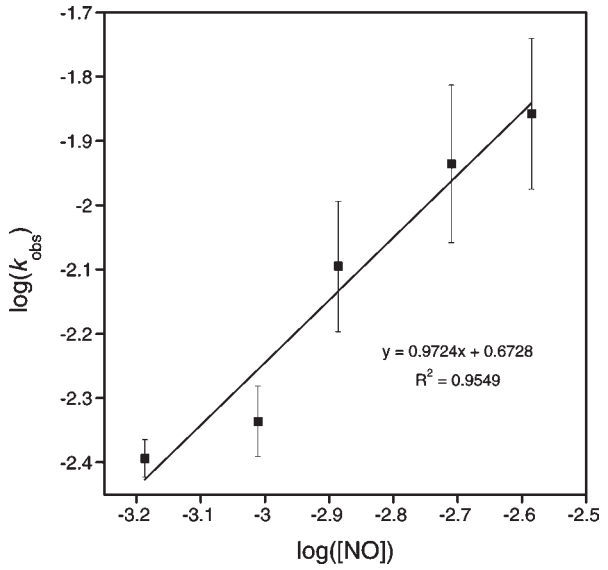

Figure 3. Plot of $\log(k_{obs})$ vs log([NO]) for the reactions of 4 μM CuFL1 with 650−2600 μM NO in 50 mM PIPES and 100 mM KCl at pH 7.0. T = 25 °C.

(650 μM NO vs 4 μM CuFL1 for the lowest [NO]). The highest NO concentration used, 2.6 mM, was at the supersaturation point,[34] and the error for the k_{obs} values therefore increased with NO concentration. However, a plot of the k_{obs} values versus the NO concentration still revealed a linear relationship, as did the corresponding log/log plot of k_{obs} versus [NO] (Figure 3). The slope of the latter revealed a first-order dependence of the reaction on the concentration of NO (1.0 ± 0.1 after linear regression analysis).

To determine the order of the reaction in [OH^-], kinetic data were collected at constant NO (650 μM) and CuFL1 (4 μM) concentrations and at constant temperature (Table 1, right-hand columns). The obtained k_{obs} values revealed a more complex pH dependence than that observed for the NO or CuFL1 concentrations. The rate constants increased with increasing pH, which is consistent with the hypothesis that deprotonation of the secondary amine of FL1 is required for reaction of CuFL1 with NO. A plot of the k_{obs} values versus [OH^-] revealed saturation behavior at high [OH^-] (Figure 4a). The plot of the k_{obs} values versus pH (Figure 4b) illustrates that, below pH 7, the observed rate constants also begin to plateau, again consistent with the hypothesis that the protonation state of the complex is crucial to progress of the reaction and formation of the N-nitrosated product. These data also provide important information about the design of new NO-specific Cu(II)-based probes. In particular, it is clear that decreasing the pK_a of the complexed secondary amine would increase the rate of reaction with NO. This feature could be valuable for biological experimentation where fast spatial and temporal resolution is required.

pH Titrations of FL1 and CuFL1. Because of the importance of secondary amine deprotonation in the reaction of CuFL1 with NO, the pK_a values of both FL1 and the CuFL1 complex were determined. Spectral changes of FL1 at different pH values were monitored by UV−vis and fluorescence spectroscopy and displayed behavior that is typical for fluorescein-based ligands (Figure 5). The fluorescence data (Figure 5a) revealed three pK_a values of 4.7 (p$K_{a(Fluor1)}$; Figure S2a in the SI), 5.6

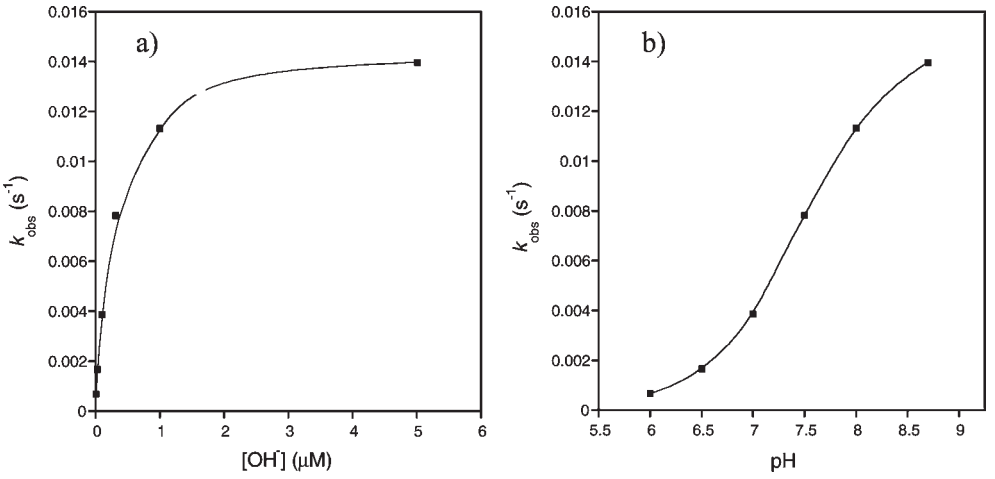

Figure 4. (a) Plot of k_{obs} vs [OH$^-$] for reactions of 4 μM CuFL1 with 650 μM NO in 50 mM PIPES and 100 mM KCl at pH 6.0−8.7. T = 25 °C. (b) Plot of k_{obs} vs pH. For both plots, lines drawn through the data are meant to clarify trends and are not mathematical fits.

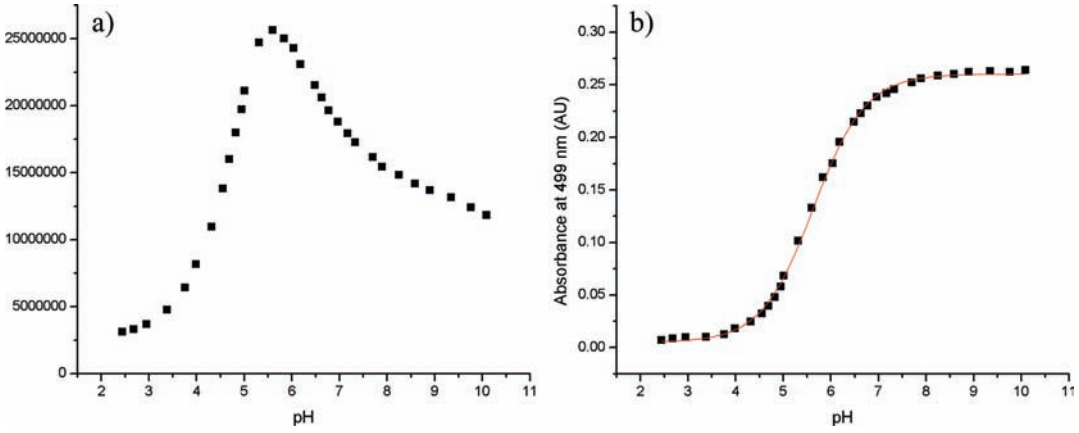

Figure 5. (a) Fluorescence emission dependence on pH, with fit, for 5 μM FL1 in 20 mM KOH and 100 mM KCl at pH ~ 12. T = 25 °C. The pH was adjusted with 6, 1, and 0.1 N HCl and 0.1 N KOH. (b) Absorbance dependence on pH. pK_a values were determined by fitting the plots of absorbance or integrated fluorescence emission at λ_{max} vs pH to the equation $y = (A_1 - A_2)/(1 + e^{(x-pK_a)/dx}) + A_2$.

(p$K_{a(Fluor2)}$), and 6.5 (p$K_{a(Fluor3)}$; Figure S2b in the SI). The p$K_{a(Fluor3)}$ value agrees well with the pK_a value of 6.1 determined by fluorescence for a related Zn(II) sensor, QZ1,[35] which was assigned to the secondary amine nitrogen atom. The p$K_{a(Fluor1)}$ value of 4.7 probably corresponds to a combination of fluorescein carboxylic acid protonation (pK_a = 4.4 for fluorescein and 3.5 for dichlorofluorescein)[36,37] and lactonization of the fluorescein. The intermediate p$K_{a(Fluor2)}$ value of 5.6 can be assigned to the quinaldine nitrogen atom (5.08 ± 0.5 for *N*,2-dimethyl-8-quinolinamine).[38] The UV−vis data are not sufficiently well resolved to determine all three pK_a values, allowing only computation of an apparent pK_a (p$K_{a(UV)}$ = 5.6; Figure 5b). The average of all three fluorescence pK_a values of 5.6 is consistent with the p$K_{a(UV)}$ value.

When the same experiment was repeated for CuFL1, the fluorescence data again revealed three pK_a values in the region of pH 2.5−9 and a fourth value above 9 that could not be adequately resolved (Figure 6a). The fluorescence data from pH 2.5 to 6.5 were fit to obtain the first value (p$K_{a(Fluor1)}$) of 4.9 (Figure S3a in the SI), the maximum revealed the second value (p$K_{a(Fluor2)}$) of 6.4, and the third value (p$K_{a(Fluor3)}$) of 7.7 was obtained by fitting the fluorescence data from pH 6.5 to 9 (Figure S3b in the SI). The UV−vis data for CuFL1, however, differed from those of FL1 in that two pK_a values were obtained (Figure 6b). Fits of the data from pH 2.5 to 5.5 (Figure S4a in the SI) and from pH 6 to 11 (Figure S4b in the SI) revealed values of 4.7 and 7.5 for p$K_{a(UV1)}$ and p$K_{a(UV2)}$, respectively. These results are in good agreement with those obtained from the fluorescence data and most likely correspond to the pK_a value for deprotonation of the secondary amine ligated to Cu(II) (7.7 and 7.5) and the pK_a value of the fluorescein bottom-ring carboxylic acid/lactonization of the fluorescein (4.9 and 4.7). The absence of a third, intermediate pK_a value in the absorbance data confirms the assignment that it belongs to the quinoline nitrogen atom, which would be bound to Cu(II) in the complex and therefore not protonated.

Activation Parameters of the Reaction of CuFL1 with NO. An Eyring analysis was performed to determine the activation parameters associated with the reaction of

(35) Nolan, E. M.; Jaworski, J.; Okamoto, K.-I.; Hayashi, Y.; Sheng, M.; Lippard, S. J. *J. Am. Chem. Soc.* **2005**, *127*, 16812–16823.
(36) Diehl, H.; Horchak-Morris, N. *Talanta* **1987**, *34*, 739–741.
(37) Leonhardt, H.; Gordon, L.; Livingston, R. *J. Phys. Chem.* **1971**, *75*, 245–249.
(38) Calculated using Advanced Chemistry Development (ACD/Laboratories) Software V8.14 (1994−2010).

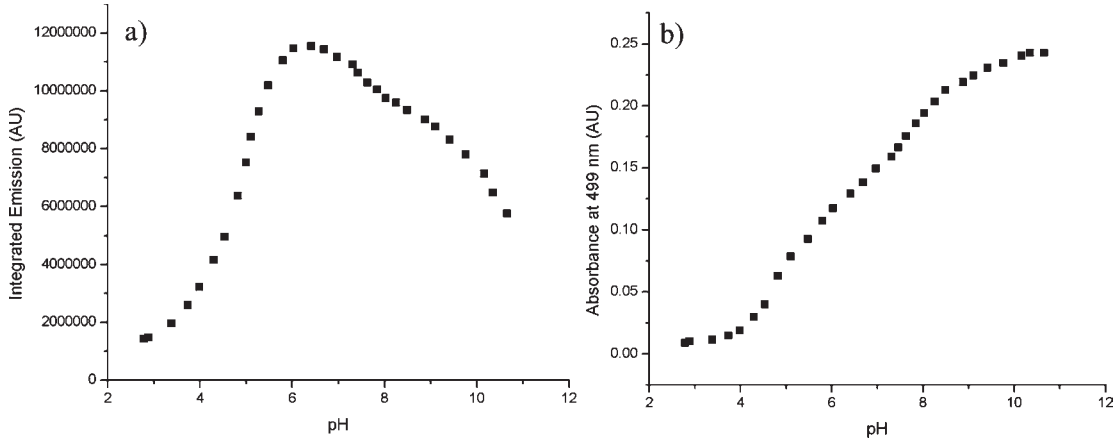

Figure 6. (a) Fluorescence emission dependence on the pH for 5 μM CuFL1 in 20 mM KOH and 100 mM KCl at pH $\sim$ 12. T = 25 °C. The pH was adjusted with 6, 1, and 0.1 N HCl and 0.1 N KOH. (b) Absorbance dependence on the pH.

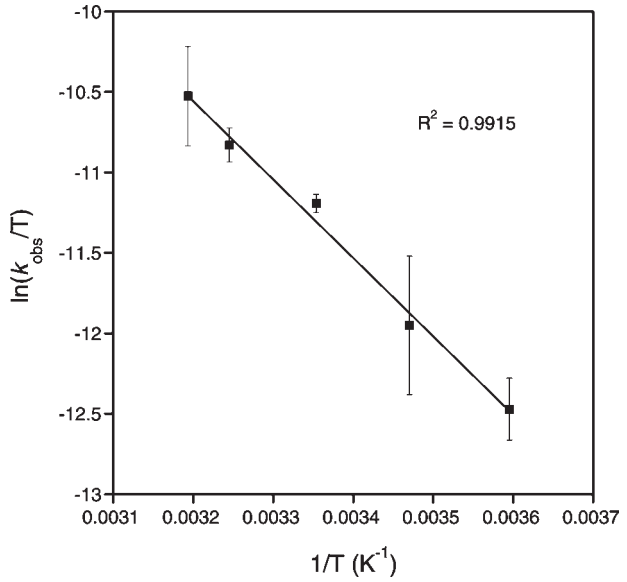

Figure 7. Eyring plot for the reaction of 4 μM CuFL1 with 650 μM NO in 50 mM PIPES and 100 mM KCl at pH 7.0. T = 278.15−313.15 K.

CuFL1 with NO (Figure 7 and Table 2). The enthalpy of activation ($\Delta H^{\ddagger}$ = 41 ± 2 kJ/mol) and activation energy (E_a = 43 ± 2 kJ/mol) indicate a relatively low activation barrier for the reaction and are consistent with values obtained from other experimental and theoretical examinations of nitrosation of secondary amines.[39−41] The negative entropy of activation ($\Delta S^{\ddagger}$ = −120 ± 10 J/mol·K) is consistent with an associative nitrosation mechanism.

pH-Dependent EPR Spectroscopy of CuFL1. EPR spectra were recorded at four pH values to determine whether the protonation state of the secondary amine affects the distribution of the unpaired electron spin density (Figure 8). At pH 4.0 the secondary amine (pK_a $\sim$ 7.5) should be fully protonated, and the observed EPR spectrum is typical of that for a rhombically distorted axial Cu(II) species with $g_{\|}$ = 2.36, $g_{\perp}$ = 2.08, and $A_{\|}$(Cu) = 463 MHz (Figure 8a). When the pH is increased to 7.0, the spectrum loses resolution but still retains axial Cu(II) character with hyperfine features. The approximate g values are $g_{\|}$ = 2.39 and $g_{\perp}$ = 2.08, and the Cu(II) hyperfine coupling constant $A_{\|}$(Cu) is ~529 MHz (Figure 8b). It is possible that broadening at pH 7.0 is observed because there is a mixture of CuFL1 and CuFL1$^-$ (see Scheme 1). At pH 10.1, however, two distinct Cu(II)-based spin-active species are observed (Figure 8c). At this pH, the ligand should be the fully deprotonated copper(II) amido species (CuFL1$^-$), and therefore the two observed species could be water- and hydroxide-bound Cu(II) complexes. Finally, at pH 12.7, ^{14}N hyperfine coupling from the nitrogen-centered radical appears to be present in the spectrum, and the Cu(II)-based species are poorly resolved (Figure 8d). Although a definitive assignment of the multiline splitting pattern resulting from significant $A(^{14}N)$ contributions is difficult, the spectrum displays features similar to those reported for a copper(I) aminyl radical species.[42] A nitrogen-centered radical would be an excellent target for attack by NO.

If a copper nitrosyl adduct were formed during the reaction of CuFL1 with NO (Scheme 2), it probably could be detected by EPR spectroscopy under conditions where the secondary amine nitrogen remains protonated. To

Table 2. Activation Parameters for the Reaction of CuFL1 with NO

T (K)	k_{obs} (s^{-1})[a,b]	
278.15	0.0011(2)	E_a (kJ/mol)[c] = 43(2)
288.15	0.0019(8)	$\Delta H^{\ddagger}$ (kJ/mol)[d] = 41(2)
298.15	0.0041(2)	$\Delta S^{\ddagger}$ (J/mol·K)[d] = −120(10)
308.15	0.0061(6)	
313.15	0.008(2)	

[a] Measurements were performed in 50 mM PIPES and 100 mM KCl at pH 7.0. T = 278.15−313.15 K, [CuFL1] = 4 μM, and [NO] = 650 μM. [b] k_{obs} values were determined by fitting the plot of absorbance at 504 nm versus time to a single-exponential equation $y = Ae^{-x/t} + y_0$. [c] $k_{obs} = Ae^{-(E_a/RT)}$. [d] $k_{obs} = (k_B T/h) \exp(\Delta S^{\ddagger} R) \exp(-\Delta H^{\ddagger}/RT)$.

(39) Casado, J.; Castro, A.; Leis, J. R.; Quintela, M. A. L.; Mosquera, M. *Monatsh. Chem.* **1983**, *114*, 639–646.
(40) González-Mancebo, S.; Calle, E.; García-Santos, M. P.; Casado, J. *J. Agric. Food Chem.* **1997**, *45*, 334–336.
(41) Zhao, Y.-L.; Garrison, S. L.; Gonzalez, C.; Thweatt, W. D.; Marquez, M. *J. Phys. Chem. A* **2007**, *111*, 2200–2205.
(42) Mankad, N. P.; Antholine, W. E.; Szilagyi, R. K.; Peters, J. C. *J. Am. Chem. Soc.* **2009**, *131*, 3878–3880.

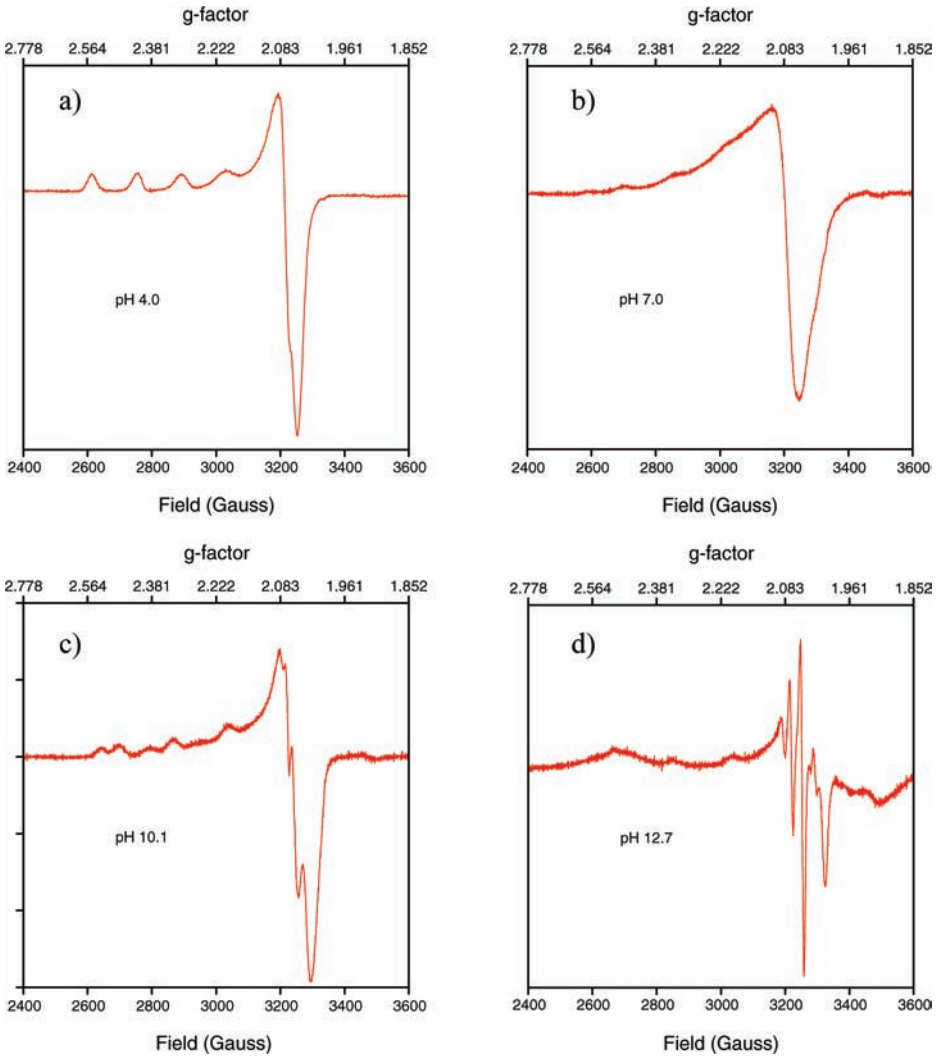

Figure 8. EPR spectra of CuFL1 at (a) pH 4.0, (b) pH 7.0, (c) pH 10.1, and (d) pH 12.7.

evaluate this possibility, NO was introduced anaerobically to solution of CuFL1 in a pH 4.0 buffer in an EPR tube, which was shaken and allowed to stand at room temperature for 13 h. The sample was then frozen, and the EPR spectrum was recorded using conditions identical to those employed to record the spectrum prior to the introduction of NO. If a CuFL1-NO adduct were formed, it would be diamagnetic, and consequently reduction of the Cu(II)-based signal intensity would be expected. The corresponding spectra, which are depicted in Figure S5 in the SI, show no changes in the EPR signal before or after NO addition, suggesting that there is no copper nitrosyl formation under these conditions.

Mechanistic Insights. On the basis of the kinetic data and activation parameters, the hypotheses for the mechanism of the reaction of CuFL1 with NO can now be examined. For the first mechanism (Scheme 1), if deprotonation were rate limiting, then the rate law would be given by eq 1. Because the kinetic data revealed the

$$\text{rate} = k_1[\text{CuFL1}][\text{OH}^-] \quad (1)$$

reaction to be first-order in [NO], mechanism 1, in the case of rate-limiting deprotonation, can be excluded. If, however, reaction of the deprotonated complex with NO were rate limiting, i.e., there is a fast pre-equilibrium between the protonated and deprotonated CuFL1, then the rate law becomes that given by eq 2. [CuFL1$^-$] can be determined from the acid−base equilibrium as defined in eq 3. Rearranging eq 3 and substituting into eq 2 yields the rate law shown in eq 4 when the reaction with NO is rate-limiting.

$$\text{rate} = k_2[\text{CuFL1}^-][\text{NO}] \quad (2)$$

$$K_{\text{eq}} = \frac{[\text{CuFL1}^-][\text{H}^+]}{[\text{CuFL1}]} \quad (3)$$

$$\text{rate} = \frac{k_2 K_{\text{eq}}[\text{CuFL1}][\text{NO}]}{[\text{H}^+]} \quad (4)$$

This rate law is consistent with the concentration dependence results. At high pH, rate saturation was observed, and under these circumstances the rate law should not depend on [H$^+$]. If mechanism 1 were operative at high pH, the rate would be limited by the reaction with NO and would be described by eq 5, which is also consistent with

the results of the concentration-dependent experiments. Therefore, mechanism 1 is viable if the reaction with NO is rate-limiting, and it also applies at high pH.

$$\text{rate} = k_2[\text{CuFL1}^-][\text{NO}] = k_2[\text{CuFL1}][\text{NO}] \quad (5)$$

The second mechanism involves an initial, reversible reaction of CuFL1 with NO to form a Cu(I)-NO^+ species, followed by deprotonation of the secondary amine and subsequent fast translocation of NO^+ to form the N-nitrosated ligand with release of Cu(I) (Scheme 2). If the reaction with NO were rate-limiting, then the rate law would be given by eq 6. Because the reaction is pH-dependent, mechanism 2 cannot be operative in the case of rate-limiting reaction with NO. If instead deprotonation of Cu(NO)FL1 were rate-limiting, then the rate law is given by that shown in eq 7, which cannot be solved analytically but is dependent on all of the reactants.

$$\text{rate} = k_1[\text{CuFL1}][\text{NO}] \quad (6)$$

If mechanism 2 were operative at high pH, the rate law would again be described by eq 5, consistent with the experimental data. Therefore, mechanism 2 is a viable mechanism if deprotonation is rate-limiting, and it would certainly apply at high pH.

$$\text{rate} = \left(\frac{k_2[\text{OH}^-]}{k_{-1} + k_2[\text{OH}^-]}\right)(k_1[\text{CuFL1}][\text{NO}] + k_{-2}[\text{Cu(NO)FL}^-][\text{H}^+]) \quad (7)$$

One can also envision alternative mechanisms involving outer-sphere electron transfer between the Cu(II) center and NO to form Cu(I)-FL1 and NO^+, followed by steps from either mechanism 1 or 2. In either of these cases, however, the reaction order in the NO concentration would most likely be greater than unity, due to scavenging of NO^+ by H_2O (eq 8), which can be ruled out by the data.

$$\text{NO}^+ + \text{H}_2\text{O} \rightleftharpoons \text{HONO} + \text{H}^+ \quad (8)$$

The pH titrations support the hypothesis that, at high pH, the reaction with NO is rate-limiting and the rate ceases to depend on $[OH^-]$. Saturation kinetics are therefore expected at pH values above the pK_a value of the Cu(II)-bound secondary amine (p$K_a \sim 7.5$), which is consistent with the observed data. The rates begin to plateau at pH ~ 8 but do not fully saturate until after at least pH 8.7, more than one pH unit above the pK_a. The activation parameters are also consistent with both mechanisms 1 and 2. The activation entropy indicates an associative rate-limiting step, which can be envisioned for either mechanism, with NO and CuFL1 coming together in the transition state. Kinetic solvent isotope effect experiments were performed in order to determine the rate-limiting step of the reaction; however, because of the protic solvent dependence of the reaction, the results were inconclusive (see the SI).

According to DFT calculations on the reaction of NO with $[Cu(DAC)]^{2+}$, the formation of a Cu(II)-NO complex is entropically disfavored and the binding is predicted to be weak.[20] On the basis of this finding and the fact that no Cu−NO stretch could be observed in an IR experiment in which $[Cu(DAC)]Br_2$ was allowed to react with NO under conditions where deprotonation of $[Cu(DAC)]^{2+}$ would not be expected, mechanism 1 was deemed to be more plausible. Because of the limited solubility of CuFL1 in acetonitrile, the analogous IR experiment could not be performed in the current system; however, EPR data from the reaction of CuFL1 and NO at pH 4.0 (vide supra) similarly indicate lack of Cu−NO adduct formation at low pH. The absence of evidence for a Cu(I)-NO species under conditions favoring proton retention of the secondary amine in FL1 does not exclude the possibility either that a Cu(I)-NO adduct can be formed at higher pH or that a Cu(I)-NO species is too short-lived to accumulate to an appreciable steady-state concentration under these conditions. We therefore do not discount formation of a Cu(I)-NO adduct as a mechanistic intermediate. The fact that the EPR spectrum changes from that of an axial Cu(II) signal at pH 4.0 to what appears to be a mixed Cu(II)-based/N-based signal at pH 12.7 suggests that, as CuFL1 is deprotonated, a nitrogen-centered radical species is formed. Such formally copper(I) aminyl species would provide a site on the ligand for NO attack. Because copper(I) nitrosyls are generally considered to be unstable,[43−45] we conclude that the reaction of CuFL1 with NO most likely proceeds by a mechanism that does not require formation of such an unstable species. Instead, we favor mechanism 1 as the preferred route.

Summary

The reaction of CuFL1 with NO in aqueous, buffered solutions is first-order in the concentration of CuFL1 and NO and also depends on the hydroxide ion concentration. Saturation kinetics occur at high base concentrations, which is consistent with deprotonation of the secondary amine of CuFL1 as a key mechanistic step. These results predict that a CuFL1-type probe with a lower secondary amine pK_a would result in a superior NO detector for in vivo applications. The activation parameters indicate an associative reaction. EPR experiments at various pH values suggest that, as CuFL1 is deprotonated, the unpaired electron density shifts from copper to nitrogen, yielding new spin-active species. Two mechanistic interpretations fit the data, with the one that invokes initial deprotonation of bound FL1 at the secondary amine followed by direct attack of NO at the deprotonated ligand being most likely.

Acknowledgment. This work was supported by Grant CHE-0907905 from the National Science Foundation. M.D.P. thanks the National Institutes of Health (NIH) for postdoctoral fellowships (5 F32 GM085930 and 1 K99 GM092970). Spectroscopic instrumentation at the MIT Department of Chemistry Instrument Facility is maintained with funding from NIH Grant NIH 1S10RR003850-01.

(43) Carrier, S. M.; Ruggiero, C. E.; Tolman, W. B. *J. Am. Chem. Soc.* **1992**, *114*, 4407–4408.
(44) Fujisawa, K.; Tateda, A.; Miyashita, Y.; Okamoto, K.-I.; Paulat, F.; Praneeth, V. K. K.; Merkle, A.; Lehnert, N. *J. Am. Chem. Soc.* **2008**, *130*, 1205–1213.
(45) Ruggiero, C. E.; Carrier, S. M.; Antholine, W. E.; Whittake, J. W.; Cramer, C. J.; Tolman, W. B. *J. Am. Chem. Soc.* **1993**, *115*, 11285–11298.

We thank Drs. Zachary Tonzetich and Neal Mankad for insightful discussions. The content is solely the responsibility of the authors and does not necessarily represent the official views of the National Institute of General Medical Sciences or the NIH.

Supporting Information Available: UV−vis spectra of the reaction of CuFL1 with NO, fits of pH titrations of FL1 and CuFL1, EPR spectra before and after NO addition at pH 4.0, and the effects of isotopic substitution on k_{obs}. This material is available free of charge via the Internet at http://pubs.acs.org.